CHARACTERISTICS OF GROUND MOTION IN NORTHERN APENNINES (LUNIGIANA-GARFAGNANA, TUSCANY, ITALY)

P. Morasca [(1)], L. Malagnini [(2)], A. Akinci [(2)],C. Eva [(1)]

[(1)] Dipartimento per lo Studio del Territorio e delle sue Risorse, Università di Genova, Viale Benedetto XV, 5, 16132 Genova, Italy.

[(2)] Istituto Nazionale di Geofisica e Vulcanologia, Viale di Vigna Murata 605, 00143 Roma, Italy.

June 2004

ABSTRACT

In this study, predictive relationships for earthquake-induced ground motion have been calibrated over the Northern Apennines. The data set used in this study consists of 605 earthquake with moment magnitudes up to 4.7, recorded by the regional seismic network, RSLG, operating in Lunigiana-Garfagnana. Regressions have been carried out using 6000 three-component short-period seismograms, all recorded within a hypocentral distance r_{max}=200 km, to empirically obtain the scaling relationships for the high-frequency S-wave motion. The dataset were used to parameterize source-spectral models, regional attenuation functions, and empirical functions of the dispersion-induced ground-motion duration. In order to obtain the regional ground-motion parameters, first of all, we regressed the logarithms of the peak values and Fourier amplitudes at a set of sampling frequencies between 0.5 and 15.0 Hz. Then, we modeled our results in terms of geometrical spreading, g(r), frequency dependent Q(f), and distance- independent average κ_0. In order to minimize the trade-off between the stress parameter and κ_0, the best value of κ_0 is searched by fitting the high frequency spectra of the small events. After obtaining κ_0, the stress parameter was calibrated on a Brune spectrum with single corner frequency on the largest events.

We also estimated the moment magnitudes using an automatic procedure that corrects each waveform for the attenuation effects and valuates the seismic moment. For the largest recorded events in the region in the last years, the automatic M_w's agree with those given by the regional CMT solutions provided by Mediterranean Network, MEDNET. Finally, we predict the absolute levels of ground shaking using the parameters, obtained in this study (source and attenuation characteristics) through the Random Vibration Theory, RVT.

INTRODUCTION

Recently a number of works have been published on the ground motion characteristics in various Italian and Mediterranean regions (Malagnini et a., 2000a, Malagnini and Herrmann 2000, Scognamiglio et al. 2004, Malagnini et al. 2002, Bay et al. 2003, Pino et al. 2001, Malagnini et al. 2000b). These authors used data from the background seismicity, and demonstrated the great importance of large amounts of observations in ground motion scaling analyses, and how the attenuation parameters vary significantly on a regional scale.

In the past, the use of national predictive relationships for the Italian territory (Sabetta and Pugliese, 1987, Sabetta and Pugliese 1996, Tento et al. 1992) might introduce uncertainties in the ground motion parameters for two reasons: i) Italy is not characterized by a single seismotectonic regime; ii) predictive relationships were usually based on the few available strong motion data. More recently, the develop of dense regional networks and the introduction of methodologies based on weak-motion recordings for purpose of producing predictive relationships (Malagnini et al. 2002), allow to reduce ground motion uncertainties through independent analysis of each tectonic and geological environment and through the use of a large amount of data. However, these results are used through the logic tree for conducting new hazard map for Italy (Working Group, 2004) in order to reduce the uncertainties on ground motion calculations.

Malagnini et al. (2000a), determined empirical attenuation relationship for the peak ground motion along the entire Apennines finding low-Q in the 0.25-5.0 Hz range and suggesting that high-frequency (1-20 Hz) seismic hazard in the Apennines may be dominated by the local seismicity. Analyzing the attenuation characteristics of the region of the 1997 Umbria-Marche earthquake, Malagnini and Herrmann (2000), confirmed the validity of the crustal attenuation parameter Q(f) proposed for the entire Apennines by Malagnini et al. (2000a), extending its validity up to 16 Hz. Although the dataset analyzed by Malagnini et al. (2000a), include few events (~5) located in the Northern Apennine, these earthquakes do not involve the Lunigiana-Garfagnana region.

One of the scopes of the present study is to calibrate a regional predictive relationship for a sector of Northern Apennines (the Lunigiana-Garfagnana) to improve the knowledge of the crustal attenuation in the area, taking advantage of the high quality and of the large amount of data (~ 600 available) recorded by the local network. Although the seismicity is generally diffuse and of relatively low energy (Solarino et al. 2002), Castaldini et al. (1998) underlined a concentration of high intensity earthquakes in correspondence of the Garfagnana tectonic depression (NW-SE directions). In the period from 1481 to 1920, the region experienced 9 earthquakes with I > 6 MCS (Imbesi et al.1987), with a maximum of intensity of 9 MCS in 1920 (Solarino 2002).

More recently the area was interested by a Md=4.9 event (October 10th, 1995) that represented a great impulse to develop a premanent seismic network (Solarino et al. 2002). The RSLG (Regional Seismic network of Lunigiana-Garfagnana) has been operating since 1999, and today we dispose of a fairly large amount of high-quality data for the region in form of a set of digital seismograms. Although preliminary studies has been carried out on the area (Solarino et al. 2002, Ferretti et al. 2002, Eva et al. 2002) a great effort is necessary to add new details to the knowledge of this interesting region. In this study we determined the attenuation characteristics together with source information in the region which are important for the seismic hazard assessment.

CRUSTAL STRUCTURE OF THE AREA

This study focuses on the regions of Lunigiana and Garfagnana, that are characterized by a complex multiple-staged history, related to the continental convergence between Africa and Europe, and to the subduction of the Adriatic lithosphere (Negredo et al. 1999, Selvaggi and Amato,1992, Ponziani et al. 1995, Rutter et al. 1980, Royden et al. 1987, Ferretti et al.2002). Three major episodes must be considered in the structural evolution of northern Apennines: the oceanic crust consumption driven by a slab dipping west, the postcollisional evolution and the opening of the Tyrrhenian sea (Cattaneo et al. 1983). We should remember that at least the earlier evolutional episodes are connected with the western Alps, since the two belts run paired with opposite structural

asymmetries (Cattaneo et al., 1983). With respect to the alpine system, however, the Northern Apennines evolution was affected by the rotation of the Corsica-Sardinia block and the opening of the Tyrrhenian sea (Ponziani et al. 1995).

The complex distribution of the seismic activity (figures 1, 2, and 3), decreasing from SE to NW (Ferretti, et al. 2002), can be ascribed to various seismogenetic structures (Cattaneo et al. 1983). These structures are related to the compressive forces associated with the collision between Africa and Europe, and responsible for the emplacement of tectonic units coming from different paleogeographic domains (Castaldini et al. 1998), and to the extensional stresses, due to the roll-back of the subducting Adria-Ionian lithosphere (Negredo et al. 1999), which gave origin to the formation of tectonic depressions like the Garfagnana (Bartolini and Bortolotti, 1971).

However, focal mechanisms, computed in the period 2000-2001 (Solarino et al. 2002), evidenced a more complex situation than just two stress domines, showing a transtensive behavior for shallow events and a compressive behavior for the few available deep events. The effect of regional focal mechanism is important because it could be reflected in the short distance scaling when vertical component observations are included in the dataset (Herrmann and Malagnini 2004).

The topography and the nature of the Moho were modified through a complex tectonic history of lithospheric stretching, astenospheric intrusions, subhorizontal shearing and isostatic uplift (Ferretti et al.2002, Ponziani et al. 1995), resulting in a patchwork of Moho pieces formed during all developments. This situation could complicate the empirical attenuation results, especially at large distances, because the change in crustal thickness could shift the effects of the supercritical reflections at the Moho to the apparent crustal propagation term at shorter or larger distances (Herrmann and Malagnini 2004).

Tomographic images obtained by Ferretti et al. 2002 highlight the presence of a high velocity zone, 3 km deep, that could be related to high velocity material connected to the Apuane roots. Also, they observed a high-velocity anomaly, diagonal in respect of the Garfagnana-Lunigiana area, at depths between 10 km and 20 km. This anomaly was explained as possible connection between different

geological conformations that distinguish the Lunigiana area from the Garfagnana. Finally, they found a lower velocity (7.5 - 7.8 km/s) zone at 40 km that could be connected to the subduction of the Adriatic plate (Ferretti et al. 2002), but the geometry of this low velocity zone is not clear because of insufficient resolution of their results, due to the distribution of deep events. In general, we expect opposite deviations between seismic velocity and attenuation characteristics because of the temperature variations. In fact, high temperatures generally indicate strong attenuation and low velocity, whereas low temperatures are generally associated to low attenuation and high velocity. For example, the typical Q_0 values for the central Apennines are in a range 100-150 (Castro et al. 1999, Malagnini et al. 2000a, Malagnini and Herrmann 2000) and the area is characterized by low-velocity anomalies (Di Stefano et al., 1999) due to the presence of hot material in the crust.

DATA SETTING

We analyzed a set of 605 earthquakes recorded by 6 stations of the RSLG network, a branch of the Regional Seismic network of Northwestern Italy, in the Lunigiana-Garfagnana region (figure 1). The stations are equipped with five-seconds, three-component seismic sensors coupled to the latest generation digital acquisition systems with a dynamic range of about 140 dB s (table 1). The development of the RSLG began in early 1998 (Ferretti et al.2002), and so our data set covers a period of 4 years starting from 1998.

The seismicity within the region is generally characterized by small events (figures 2A and 2B) whose local magnitudes are usually lower than 2.5 as shown in figure 2B. However, the area is a potential source of high energy events as demonstrated by many historical events (Camassi and Stucchi 1996). Almost all earthquakes are located in the shallow crust (figure 2D). The cross sections in figure 3 show a clear increase of focal depths from SW to NE. This behavior was observed by Cattaneo (1983), and by Di Stefano et al. (1999), who interpreted the deepening of the seismicity of the external zones (toward the Adriatic sea) deeper than the seismicity of the internal

one (Tyrrhenian), as a consequence of the subduction of the Adriatic lithosphere beneath the Apennine chain (Cattaneo 1983, Di Stefano et al. 1999.

The events in our data set were selected based on their signal-to-noise ratios, computed on the available seismograms in a frequency band 2-11 Hz (figure 4) and recorded by at least 2 stations. The source - receiver hypocentral distance distribution for the whole dataset is shown in figure 5.

Station	coordinates	Sensor	Acquisition system	Since
BACM	44N 16.73 10E 04.39	LennartzLE-3D/5s	Mars88 Modem	17/11/1998
CODM	4N 21.31 09E 49.98	LennartzLE-3D/5s	Mars88 Modem	10/03/1999
GRAM	44N 29.47 10E 03.95	LennartzLE-3D/5s	Mars88 Modem	21/04/1999
SARM	44N 11.09 10E 24.09	LennartzLE-3D/5s	Mars88 Modem	20/03/1998
SCUM	44N 24.98 09E 32.23	LennartzLE-3D/5s	Mars88 Modem	13/11/1998
VINM	44N 09.13 10E 29.49	LennartzLE-3D/5s	Mars88 Modem	30/09/1998

Table 1. The three-component stations used in this study.

REGRESSION ANALYSIS AND RESULTS

The methodology, used in this study, is well consolidated as confirmed by the accurate analysis of many critical aspects described by Herrmann and Malagnini (2004). A detailed description about the approach can be found in previous works as well (Raoof et al. 1999, Malagnini and Herrmann 2000, Malagnini et al. 2000a, Malagnini et al. 2000b, Pino et al. 2001, Malagnini et al. 2002).

The essence of the method is to filter each time history around a set of sampling frequencies (f_{0i}) using a cascade of an 8 pole Butterworth high pass filter at $f_c = f_0/1.414$ Hz and an 8 pole Butterworth low pass filter at $f_c=f_0*1.414$ Hz. After filtering, the maximum amplitudes of the bandpass-filtered waveforms are measured for the time domain analysis. For the frequency domain analysis, the rms average of the Fourier amplitude spectrum of the original waveform is measured between the corner frequencies of the specific bandpass filter for each seismogram and each central frequency. Finally, two sets of regressions are run on the peak amplitudes of the filtered time histories, and on the Fourier spectral amplitudes, for source ($SRC_i(f_c,r_{ref})$), path (attenuation, $D(r_{ij}, r_{ref}, f_c)$), and site terms ($SITEj(f_c)$) through:

$$A_k (f_{c,} r_{ij}) = SRC_i(f_c,r_{ref}) + SITEj(f_c) + D(r_{ij}, r_{ref}, f_c) \quad (1)$$

The term on the left-hand-side of (1) is the logarithm of the observed amplitude value measured on the k-th filtered seismogram.

Regressions are performed in the L_1-norm since it is less sensitive to large outliers than a classic least-squares one. During the regressions, some constraints are applied to reduce the degrees of freedom of the system, such as forcing $D(r_{ref})= 0$ at the reference distance of 40 km. This particular reference distance has been chosen large enough that errors in source depth will not be significant, and not too large that the distance at which supercritical reflections from the Moho could complicate the motion (Herrmann and Malagnini, 2004). Another constrain is taken over the site terms, such as $SITE_{BACM}$ (f) + $SITE_{GRAM}$ (f) + $SITE_{SCUM}$ (f) + $SITE_{SARM}$(f) = 0 because of the stations are characterized by neglectable amplification effects (Eva et al 2002). Finally, a smoothing constraint has been applied to D(r) in order to reduce the effect of possible gaps in distances.

The consequence of these constraints, the excitation term is the expected motion at the average site among these 4 stations, at the 40 km distance from the source.

After the inversions, our empirical estimates of the crustal attenuation are modeled through the use of Random Vibration Theory (RVT, Cartwright and Longuet-Higgins,1956) and of:

$$D(r,r_{ref},f_c) = \log g(r) - \log g(r_{ref}) - \frac{\pi f_c (r - r_{ref})}{\beta Q_0 (f / f_{ref})^{\eta}} \log e \quad (2)$$

where r is the hypocentral distance, f_c is the central frequency of the filter, and r_{ref} is a reference hypocentral distance of 40 km.

The excitation terms obtained from the regressions are modeled using the following functional form:

$$exc(f,r_{ref}) = C(2\pi f) M_0 s(f) g(r_{ref}) \exp\left[- \frac{\pi r_{ref}}{\beta Q_0 (f / f_{ref}) \eta} \right] v(f) \exp(-\pi f k_0) \quad (3)$$

where:

$$s(f) = \frac{1}{1 + \left(\frac{f}{fc}\right)^2}$$

$$C = (0.55)(0.707)(2.0) / 4\pi\rho\beta^3$$

$\nu(f)=1.0$

A term $\exp(-\pi k_0 f)$ is used in order to fit the high-frequency spectral shape of the excitation terms.

a) Duration

We quantify the duration of the ground motion as a function of frequency and hypocentral distance, which is used to estimate the expected motions using the RVT. We choose to compute signal duration using the definition given by Raoof et al. (1999), since it is consistent with RVT. Duration is obtained by integrating the square of the filtered ground velocity, and measuring the time window between 5-75% of the integral seismic energy following the S-wave arrival. Figure 6 illustrates the duration measurements for all data at some central frequencies. It is clear that the measured durations are influenced by scattering effects, especially at low frequencies, to the difficulty in defining the window length because of signal noise. An L1-norm minimization has been chosen to define the curves again because of its poor sensitivity to the large outliers. The results show an increase of duration with distance due to crustal structure and a weak frequency dependence.

b) Regional Attenuation

We model our results in terms of geometrical spreading, g(r), frequency dependent Q(f), and distance-independent average κ_0. Figure 7 shows the attenuation term D(r) in time (7a) and frequency (7b) domain, as obtained from regressions (color curves), and the model described by the equation (2) (black curves). Best fit is obtained using following parameters for Q and its frequency dependence as well as geometrical coefficients as a function of distance

$$Q(f) = 180\, f^{0.35} \qquad (4)$$

$$g(r) = \begin{cases} r^{-1.2} & r \le 15 \\ r^{-1.0} & 15 < r \le 30km \\ r^{+0.3} & 30 < r \le 50km \\ r^{+0.2} & 50 < r \le 60km \\ r^{-1.5} & 60 < r \le 80km \\ r^{-0.5} & r > 80km \end{cases} \qquad \text{for} \quad f \le 6 \text{ Hz} \tag{5}$$

$$g(r) = \begin{cases} r^{-1.2} & r \le 15 \\ r^{-1.0} & 15 < r \le 30km \\ r^{+0.4} & 30 < r \le 50km \\ r^{+0.3} & 50 < r \le 60km \\ r^{-1.6} & 60 < r \le 80km \\ r^{-0.6} & r > 80km \end{cases} \qquad \text{for} \quad f > 6 \text{ Hz}$$

In figure 7 we plot the deviation from 1/r of the attenuation terms, in order to enhance the frequency dependence of D(r,f). The empirical distance terms are parameterized as a piecewise linear function with 13 nodes between 10 and 160 km. Nodes have been chosen by examining the distribution of data with distance to have stable regressions. At 40 km from the hypocenter, D(r) is zero because of the constraint applied during the regression, implies that the excitation term defines the ground motion level at that distance.

In figure 7, the geometrical spreading shows weak frequency dependence, but a significant distance dependence. Generally the expected geometrical spreading coefficient at near source distances is $r^{1.0}$ since the waves travel upward from the source to the site (dominates direct waves). However, in our case it is attenuating slightly faster than $r^{1.0}$, reflects that the duration is increasing with distance (Herrmann and Malagnini 2004). At regional distances, the expected geometrical spreading coefficient simply becomes 0.5 since it is dominated by Lg-phases. Finally, at intermediate distances the geometric attenuation function is complicated by a combination of direct arrivals and supercritical reflections at the crustal interfaces and especially at the Moho. It is interesting to observe the effects of decrease in geometrical attenuation between 30 and 60 km of distance.

Similar results were obtained by Bay et al. 2003 for Switzerland in a distance range between 70 and 100 km, and explained in terms of reflections of shear waves at the Moho.

c) Source Excitation Modeling

A comparison between our observed excitation terms at 40 km and the model based predictions (equation 3) is shown in figure 8. The parameters of the Brune spectrum are shown in table 2. The stress parameter $\Delta\sigma$ is a kind of scale parameter/value which defines the spectral shape and the levels of the empirical excitation terms. In figure 8 the empirical results are represented by thin black lines and the theoretical curves by thick gray lines.

The attenuation parameter, κ_0, in equation (3), indicates site-specific attenuation properties at high frequency. In our case, it represents a regional average value between the sites, those the sum was constrained to be zero. In order to minimize the trade-off between the stress parameter and κ_0, we first searched for the best value of κ_0 by fitting the high frequency spectra of the small events. After obtaining κ_0=0.02, the stress parameter was calibrated on the largest events, obtaining a value of 10 MPa for an event with moment magnitude 4.0.

A small number of events (around 30) show different excitation terms that can not be fitted with the evaluated stress-attenuation parameters (see figure 9). We found that most of these events are located S-SE of the Lunigiana - Garfagnana region (figure 10), and connected to the structural and geological setting of the Tuscany. For the future, it will be interesting to integrate these events with a large data set from earthquakes located in Tuscany and to derive the attenuation parameters for the region separately. The large differences in spectral shape, however, might be due to the different attenuation experienced by seismic waves along their paths outside the Garfagnana and coupled to different source characteristics.

Figure 11 illustrates the final residuals of the time domain regressions computed for each sampling frequency. In each case we observe a gaussian distribution with few large outliers. As expected for the frequency domain, the final residuals are larger (figure 12) because of higher noise levels in the Fourier amplitude spectra, with respect to the more stable peak amplitudes.

Table 2

ρ	2.8 g/cm3
β	3.5 km/sec
$\Delta\sigma_{(Mw= 4.1)}$	50 MPa
f_c	$4.9 \times 10^6 \beta(\Delta\sigma/M_0)^{1/3}$ Hz
k_0	0.02 sec
$\nu(f)$	1.0

Parameters of the Brune Spectrum used to compute the theoretical excitation terms

d) Site Terms

Inverted site terms relative to horizontal ground motion (figure 13) represent the deviation from the average among the following stations (BACM, GRAM, SCUM, SARM). Only sites with "stable" behavior were included in the site constraints (all results must be associated with this average site term). The site effects are revealed in the 0.5-5 Hz frequency for the VINM station, which was not constraint to 0.0 since its amplification on the horizontal components would have influenced the average. Our results are in agreement with previous studies (Eva et al., 2002), that very small amplification effects were noted for BACM, GRAM, SCUM and SARM, while the amplification picks were observed for CODM between 4 and 9 Hz and for VINM around 2 Hz.

MOMENT MAGNITUDES

An automatic procedure proposed by Malagnini et al. (2004) has been used to compute seismic moments of the events in our data set. The method uses the attenuation parameters calibrated for a region to correct event spectra and then estimates the seismic moments from the rms-average of the flat portion of the corrected spectra. In order to obtain the moment magnitudes we used Hanks and Kanamori (1979) relation and compare our results with the one obtained independently given by MedNet (MEDiterranean NETwork). Because the period of our data set was short (1998-2001) we were able to analyze only few events with magnitudes of Sept. 14th 2003, $M_{w,\ MedNet}$ = 5.3, June 8th

2002, $M_{w,\ MedNet}$ = 4.2, and June 18th 2002, $M_{w,\ MedNet}$ = 4.3. As it is seen in table 3 our results are comparable with those given by MedNet (see table 3). Figure 14 we also show our automatic seismic moments versus local magnitudes, which are given by Ferretti et al. (2002a).

Table 3

EVENT	MedNet M_W	AUTOMATIC M_W
030914214316	5.3	5.2
020608201322	4.2	4.4
020618222354	4.3	4.3

PREDICTION OF REGIONAL GROUND MOTION

After the evaluation of source-spectral models (Brune, 1970, 1971), regional attenuation functions, and empirical functions of the dispersion-induced ground-motion duration (table 2) it was possible to predict the absolute levels of ground shaking for the region. In order to do that we used random vibration theory following Boore's (1996) implementation of the stochastic ground motion model (Boore's SMSIM codes). This method is well known and useful for obtaining ground motions at frequencies of interest to engineers and for regions where the large earthquake recordings are not available. Moreover, the simulated earthquake motions can be used to overtake the difficulties due to the lack of recorded motions extending the ground motion predictions up to higher magnitudes.

Theoretical computation of peak ground acceleration (PGA), shown in figure 15 have been derived by the SMSIM codes combined with excitation and crustal attenuation parameters produced by this study. Figure 15 also shows a comparison between the attenuation relations by Malagnini et al. (2002) for the eastern Alps, Malagnini et al. (2000) for the Apennine, and Morasca et al. (2004) for the western Alps with AMB96 and SP96. The predicted peak horizontal accelerations of AMB96 and SP96 are very similar to Malagnini et al., (2000, 2002) and Morasca et al. (2004) predictions in the distance range, 20-200 km in the Apennines and Western Alps, while they are lower in the Eastern Alps between 0-70 km distance ranges and higher beyond 70 km.

It is important to note that the comparison with Ambraseys et al. (1996) is an approximation since their results are in terms of fault distance and ours in terms of epicentral distance. Except for short distances, our model predicts a more rapid decrease of motion with distance than Ambraseys et al. (1996) and Sabetta and Pugliese (1996). As evidenced by Douglas 2002, it is not simple to compare ground motion estimations from different works because of many variable factor such as geological and seismotectonical conditions, data selection and methods. Predictive relationships by Ambraseys (1996) and Sabetta and Pugliese (1996), are based on European and Italian strong-motion data that none of them are located in our studied area. Consequently, the use of their relationships to predict ground motion in the Lunigiana-Garfagnana region could represent an approximation since the regional characteristics are not taken into account adequately.

Moreover, different methods and magnitude definition have an influence into ground motion estimations. Ambraseys (1996) refers to M_S, while Sabetta and Pugliese (1996), use M_S for large events (M>5.5) and M_L for smaller earthquakes. In our study we use M_W and the same method applied in the Eastern Alps (Malagnini et al. 2002), Western Alps (Morasca et al. 2004) and Apennines (Malagnini et a., 2000a). Consequently differences in the comparison with these regions may be ascribed to the different geological and structural characteristics.

CONCLUSIONS

Based on regression analysis over a data set of ground velocities from three-component recordings, we describe attenuation characteristics of the Lunigiana - Garfagnana region, the Tyrrhenian side of north-western Apennines. The frequency dependent quality factor Q(f) and the geometrical spreading have been specified by fitting our data assuming $Q(f)= Q_0 f^{\eta}$ and a piecewise-linear geometrical spreading function.

Comparing our results with previous studies on the Apennines (Castro et al. 1999, Malagnini et al., 2000a, Rovelli et al. 1988), we should not necessarily expect the same results because in this study we analyze a small sector of a complex structure, while the results obtained by Castro et al. 1999

refers to central Apennines, and the ones given by Malagnini et al. (2000a) and Rovelli et al. (1988) represent an average over the entire Apennine chain particularly focus on the Central and Central-Southern Apennines. However, the Q_0 parameter obtained for the Lunigiana-Garfagnana region is just slightly higher than the typical values given by Castro et al. (1999), Malagnini et al., (2000a), Rovelli et al. (1988). Besides that the geometrical attenuation function used to reproduce the observed attenuation shows important features of the Lunigiana-Garfagnana structures. Variations in the crustal thickness (depth to the Moho) and in the position (depth) of intra-crustal interfaces have the strongest influence in the geometrical spreading, because they determine the distance of reflected phase arrivals (Herrmann and Malagnini, 2004). For the Lunigiana and Garfagnana we found a complicated geometrical spreading function which is influenced by a combination of direct and supercritically-reflected arrivals. This might be explained as the effect of an inhomogeneous Moho, modified by complex processes during the evolution of the Northern Apennines (Ferretti et al., 2002).

Analyzing our data set, we found some differences in the excitation terms derived from events located in the area S-SE of Lunigiana-Garfagnana. These could be related to the structural differences between this region and the southern area. In fact, Lunigiana-Garfagnana region is likely to be characterized by crustal heterogeneous (Cattaneo et al. 1986), like strong anisotropy and irregularities due to the presence of the Apuane metamorphic structure in the southern area. Future studies are needed in order to study the attenuation characteristics of Tuscany, and to compare the results with the small sector of Northern Apennines analyzed in the present paper.

For the studied region, finally, we determined new predictive ground motion relationship taking into account properties of the source excitation and of the crustal structure, and their effect on wave propagation. The differences in wave propagation can thus be easily linked with the geologic and tectonic settings of the areas and play a key role in hazard studies.

ACKNOWLEDGMENTS

This work was performed under the auspices of the Italian Ministry of University and Scientific Research (MIUR), under FIRB contract no RBAU013NRZ. Additional support was obtained in the framework of the project "Probable Earthquakes in Italy from Year 2000 to 2030", funded by the Gruppo Nazionale per la Difesa dai Terremoti.

REFERENCES

Ambraseys, N. N., Simpson, K. A., and J. J. Bommer . Prediction of horizontal response spectra in Europe. *Earthquake eng. Struct. Dyn.* **25**, 371-400, 1996

Anderson, J. G., and S. E. Hough (1984). A model for the shape of the Fourier amplitude spectrum of acceleration at high frequencies. *Bull. Seism. Soc. Am. 74, 1969-1993.*

Bartolini, C., Bortolotti, V. (1971). Study di geomorfologia e neotettonica, 1. I depositi continentali dell'Alta Garfagnana in relazione alla tettonica plio-pleistocenica. *Mem. Soc. Geol. It. 10, 203-245*.

Bay, F., Fäh D., Malagnini, L. and D. Giardini (2003).Spectral Shear-Wave Ground-Motion Scaling in Switzerland. . *Bull. Seism. Soc. Am. 93 (1), 414-429.*

Boore, D. M. (1996). SMSIM- Fortran programs for simulating ground motion from earthquakes: version 1.0, *U.S.Geol. Surv. Open-File Rept*.96-80-A, 73 pp.

Boore, D. M. (2000). Prediction of Ground Motion using the Sthocastic Method. *Aki Symposium, PAGEOPH, vol.* 1.1.

Brune, J. N. Tectonic stress and the spectra of seismic shear waves from earthquakes. *J. Geophys. Res.,* **75**, 4997-5009, 1970.

Camassi, R. and Stucchi, M. (1996). NT4.1 A Parametric Catalogue of Damaging Earthquake in the Italian Area. *CNR-GNDT, Milano, 65 pp.*

Cartwright, D.E., Longuet-Higgins (1956): The statistical distribution of the maxima of a random function. *Proc. Roy. Soc. London A 237, 212-232.*

Castaldini, D., Genevois, R., Panizza, M., Puccinelli, A., Berti, M., Simoni, A. (1998): An

integrated approach for analysing earthquake-indiced surface effects: a case study from the Northern Apennines, Italy. *J. Geodynamics Vol. 26 No. 2-4, pp. 413-441.*

Castro, R. R., Monachesi, G., Mucciarelli, M., Troiani, L. (1999) P - and - S –wave attenuation in the region of Marche, Italy. *Tectonophysics* **302**, 123-132.

Cattaneo, M., Eva, C., Giglia, G., Merlanti, F. (1983) Seismic Hazard in the Northwestern Apennines. *Pageoph Vol. 121, No 2.*

Cattaneo, M., Eva, C., Giglia, G., Merlanti, F. (1986): Pericolosita' sismica della Garfagnana. In: *Progetto Terremoto in Garfagnana e Lunigiana. Ed. Imbesi, Marcellini, Petrini, Di Passio, Ferrini. CNR – GNDT – Regione Toscana, Firenze.*

Decandia, F. A., Lazzaretto, A. Lotta, D., Cernobori, L., Nicolich, R. (1998). The CROP 03 traverse: insights on post-collisional evolution of Northern Apennines. *Mem. Soc. Geol. It. 52, 427-439.*

Di Stefano, R., Chiarabba, C., Lucente, F., Amato, A. (1999). Crustal and uppermost mantle structure in Italy from the inversion of P-wave arrival times: geodynamic implications. *Geophys. J. Int. 139, 483-498.*

Eva, C., Carenzo, G., Ferretti, G., Pasta, M., Solarino, S., Spallarossa, D., Zumino, E.(2002). Integrazione alla rete sismica locale di tipo sismometrico in Garfagnana e Lunigiana, correlazioni sismotettoniche, definizione delle aree sismogenetiche, proposta di legge di attenuazione sismica dell'area e determinazione dei parametri di amplificazione locale di un centro urbano. *Convenzione tra Regione Toscana e DIP.TE.RIS.*

Ferretti, G., Solarino, S., Eva, E. (2002): Crustal structure of the Lunigiana-Garfagnana area (Tuscany, Italy): seismicity, fault plane solutions and seismic tomography. *Bollettino di Geofisica Teorica ed Applicata*, **43**(3-4): 221-238.

Ferretti, G., Spallarossa, D., Solarino, S., Eva, C. (2002a). A local magnitude scale for the regional network of Lunigiana-Garfagnana (Tuscany, Italy). *Poster presentation at ESC 2002.*

Hanks, T. C. Kanamori, H. (1979). A moment magnitude scale. *J. Geophys. Res. 84, 2348-2350.*

Herrmann, R. B., Malagnini, L. (2004) Interpretation of high frequency ground motion from Regional Seismic Network Observations. *Bull. Seism. Soc. Am.(submitted)*

Imbesi, G., Marcellini, A., Petrini, V., Di Passio, C.,Ferrini, M. (1987): Progetto terremoto in Lunigiana-Garfagnana. *CNR-GNDT. Regione Toscana. Ed. La Mandragora pp. 1-151 Firenze.*

Kramer, S. L. (1996). Geotechnical earthquake engineering. *Prentice Hall, Upper Saddle River, NJ 07458, 653.*

Malagnini, L., Akinci, A., Herrmann, R.B., Pino, N. A., Scognamiglio, L. (2002): Characteristics of the ground motion in northeastern Italy. *Bull. Seism. Soc. Am., 92, 6, 2186-2204.*

Malagnini, L., Herrmann, R. B. (2000): Ground-motion scaling in the Region of the 1997 Umbria-Marche Earthquake (Italy). *Bull. Seism. Soc. Am. 90, 1041-1051*.

Malagnini, L., Herrmann, R. B., Di Bona, M. (2000a): Ground-motion scaling in the Apennines (Italy). *Bull. Seism. Soc. Am. 90, 1062-1081*.

Malagnini, L., Herrmann, R.B., Koch, K. (2000b): Regional Ground-Motion Scaling in Central Europe. *Bull. Seism. Soc. Am., 90, 1052-1061.*

Morasca, P, Malagnini, L., Akinci, A., Spallarossa, D., Ground-motion scaling in the western Alps. *J. of Seismology (submitted),* 2004.

Negredo, A. M., Barba.,S. Carminati, E.,Sabadini, R., Giunchi, C. (1999): Contribution of numeric dynamic modelling to the understanding of seismotectonic regime of the northern Apennines. *Tectonophysics 315, 15-30.*

Pino, N.A. Malagnini, L., Akinci, A., Scognamiglio, L., Herrmenn, R.B., Stavrakakis, G., Chouliaras, G. (2001): Ground Motion Scaling relationships for mainland Greece and Crete.
Seism. Res. Lett., 72, 258.

Ponziani, F., De Franco, R., Minelli, G., Biella, G., Federico, C., Pialli, G. (1995) Crustal shortening and duplication of the Moho in the Northern Appenines: a view from seismic refraction data. *Tectonophysics 252, 391-418.*

Raoof, M., Herrmann, R.,B., Malagnini, L., (1999): Attenuation and excitation of three-component

ground motion in Southern California. *Bull. Seism. Soc. Am. 89, 888-902*

Rovelli, A., Bonamassa, O., Cocco, M., Di Bona, M., Mazza, S. (1988). Scaling laws and spectral parameters of the ground motion in active extensional areas in Italy. *Bull. Seism. Soc. Am.78, 530-560.*

Royden, L., Patacca, E., Scandone, P. (1987): Segmentation and configuration of subduvted litosphere in Italy: an important control on thrust-belt and foredeep-basin. *Geology, 15,714-717.*

Rutter, K. J., Giese, P., Closs, H. (1980): Litospheric split in the descending plate: observations from the Northern Apennines. *Tectonophysics 64, T1-T9.*

Sabetta, F., and A. Pugliese (1987). Attenuation of peak horizontal acceleration and velocity from Italian strong-motion records. *Bull. Seism. Soc. Am.* **77**, 1491-1511.

Sabetta, F., and A. Pugliese. Estimation of response spectra and simulation of nonstationary earthquake ground motion. *Bull. Seism. Soc. Am.* **86**, 337-352. 1996.

Scognamiglio L., Malagnini, L., A. Akinci. (2004). Ground Motion scaling in Eastern Sicily (Italy). *Bull. Seism. Soc. Am.* (submitted).

Selvaggi, G., Amato, A. (1992): Subcrustal earthquakes in the Northern Apennines (Italy): evidence for still active subduction? *Geoph. Res. Lett. Vol. 19, N 21, pp. 2127-2130.*

Solarino, S. (2002): The September 7, 1920 earthquake in Lunigiana-Garfagnana (Tuscany, Italy): can instrumental data provide a reliable location? (*Proceedings of the XXVIII Assembly of ESC, cd-rom)*

Solarino, S., Ferretti, G., Eva, C. (2002): Seismicity of Garfagnana-Lunigiana (Tuscany, Italy) as recorded by a network of semi-broad-band instruments. *Journal of Seismology 6, 141-152*.

Tento, A., Franceschina, L. and Marcellini, A. (1992). Expected ground motion evaluation for Italian sites. Proceedings of the "Tenth World Conference on Earthquake Engineering", Madrid, Spain, 19-24 July, 1992, Vol 1, pp. 489-494.

FIGURES CAPTIONS

Figure 1 – Map showing location of the earthquakes (circles) used in the present study, relative to RSLG stations (triangles).

Figure2 - Characteristics of the seismicity included in the database of waveforms used in this study: (A) distribution of local magnitudes (given by Ferretti et al. 2002a) with respect to hypocentral distance; (B) number of recordings as a function of local magnitude; (C) hypocentral distance distributions of the waveforms; (D) distribution of recorded events with respect to the depths.

Figure3 - Seismic cross-sections through the Lunigiana-Garfagnana region: the three sections (AB, CD, EF) show a deepening of the earthquakes from south-west toward north-east.

Figure 4 – Signal-to-noise ratios calculated in the frequency band 2-11 Hz. S/N ratios are plotted separately for events of local magnitude lower and higher than 3.

Figure 5 – Source –receiver distribution of the events for each station used in this study.

Figure 6 – Estimates of duration computed on each seismogram (dark small dots) and L1-norm estimates of the duration function (light-gray diamonds linked by piecewise linear curves) versus hypocentral distance, at a series of sampling frequencies.

Figure 7 – Inverted attenuation terms ($D(r,r_{ref},f)$) on the peak amplitudes (A) and on the Fourier amplitudes (B) obtained for the Lunigiana-Garfagnana region (color lines), and theoretical estimates (black curves). For plotting purposes, attenuation curves have been normalized to zero at a reference distance of 40 km. Consequently, the horizontal dashed line plotted in each frame indicates an attenuation proportional to 1/r.

Figure 8 – Inverted excitation terms (black diamonds linked by thin black lines) and theoretical curves (thick gray lines) predicted for different moment magnitudes. Frame (A) refers to peak-filtered velocities, frame (B) refers to Fourier amplitude spectra.

Figure 9 - Inverted excitation terms (black diamonds linked by thin black lines) of some events that show a different behavior with respect to the most of the events included in our dataset. Frame (A)

refers to peak-filtered velocities, frame (B) refers to Fourier amplitude spectra. The difference is evidenced in both frequency and time domain analysis.

Figure 10 – Epicentral locations of the events with a different behavior with respect to the most of the events included in our dataset (circles). Most of them are located at E- SE relative to RSLG network.

The tectonic sketch derives from http://www.geology.yale.edu/~brandon/RETREAT/Proposal/

Figure 11 – Histograms of the residuals computed in the regressions over the peak amplitudes for each sampling frequency. The use of an L1-norm minimization scheme eliminates the effects of the non-Gaussian large tails of residuals.

Figure 12 - Histograms of the residuals computed in the regressions over the Fourier amplitudes for each sampling frequency. The use of an L1-norm minimization scheme eliminates the effects of the non-Gaussian large tails of residuals.

Figure 13 - Site terms obtained from the regressions on peak velocities (A) and on Fourier amplitudes (B).

Figure 14 - Our seismic moments versus Ml for all earthquakes in the data set and for some large events recorded in the region after 2001.

Figure 15 – Peak ground acceleration (PGA) for magnitude 5 and 6. Our results are compared with the PGA relations for the eastern Alps (Malagnini et al., 2002), the Apennine (Malagnini et al. 2000), the western Alps (Morasca et al. 2004) and with Sabetta and Pugliese (1996), and Ambraseys et al. (1996).

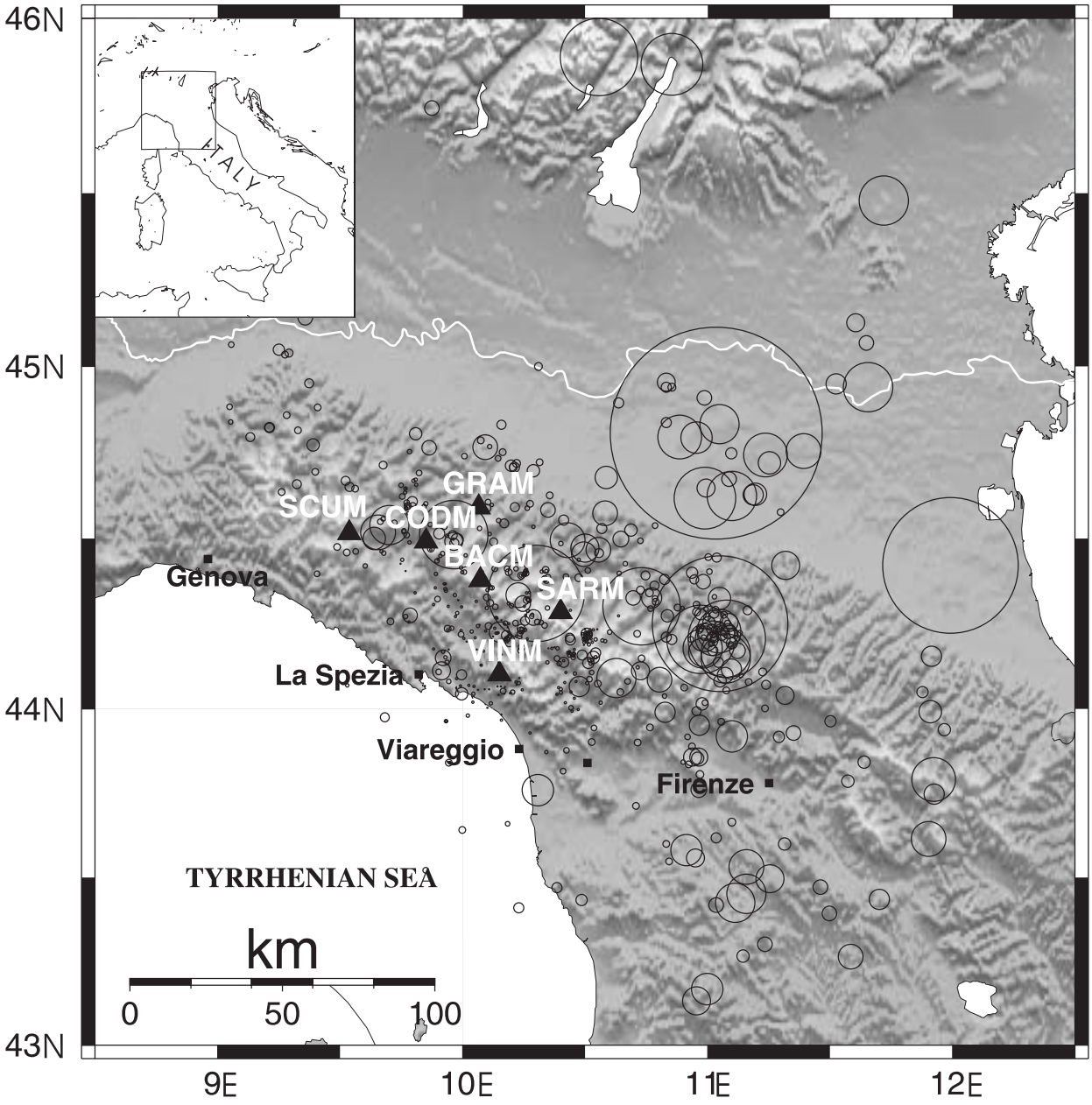
46N
45N
44N
43N
9E
10E
11E
12E
ITALY
GRAM
SCUM
CODM
BACM
SARM
VINM
Genova
La Spezia
Viareggio
Firenze
TYRRHENIAN SEA
km
0
50
100

Figure 1

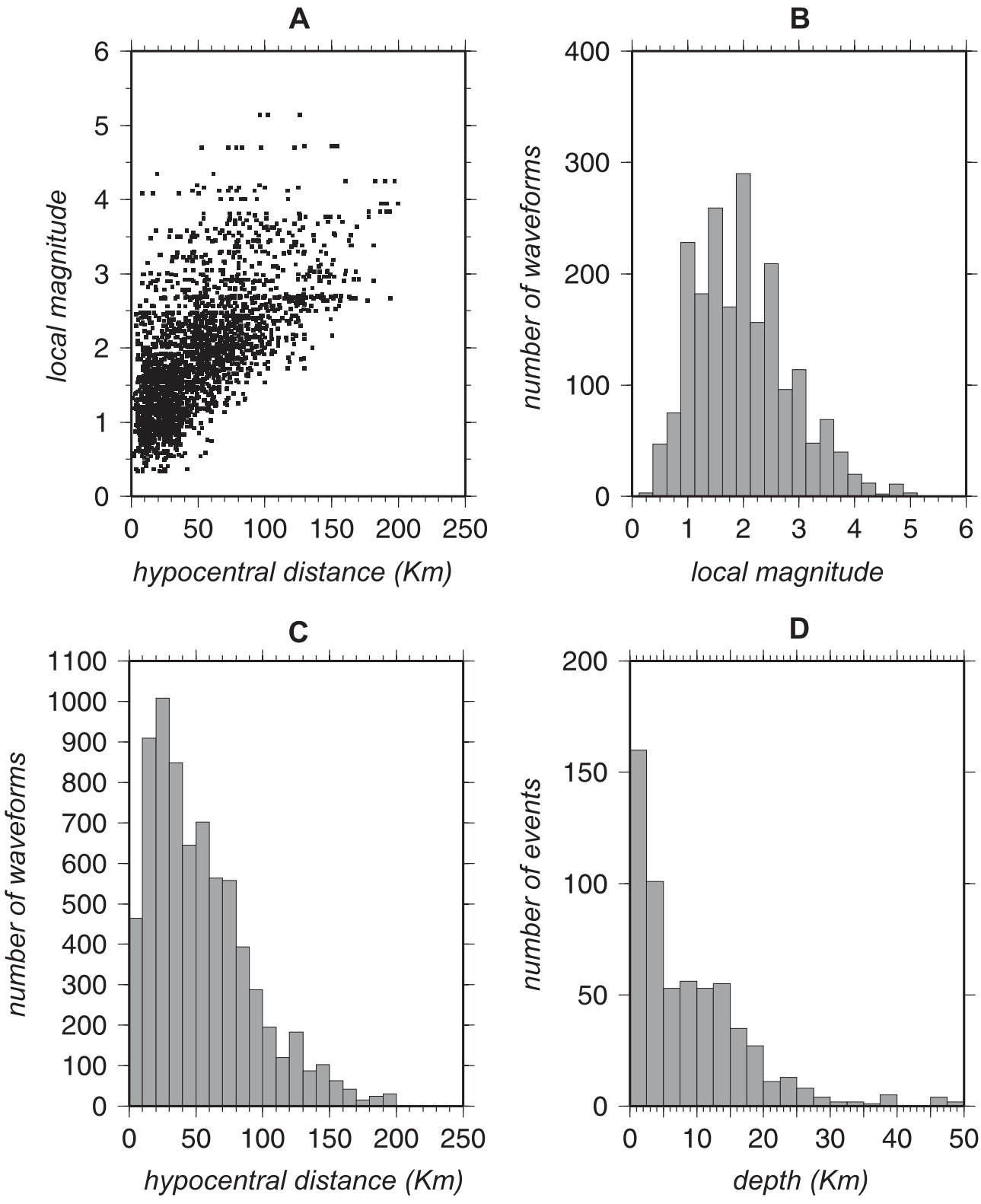
A
local magnitude
hypocentral distance (Km)
B
number of waveforms
local magnitude
C
number of waveforms
hypocentral distance (Km)
D
number of events
depth (Km)

Figure 2

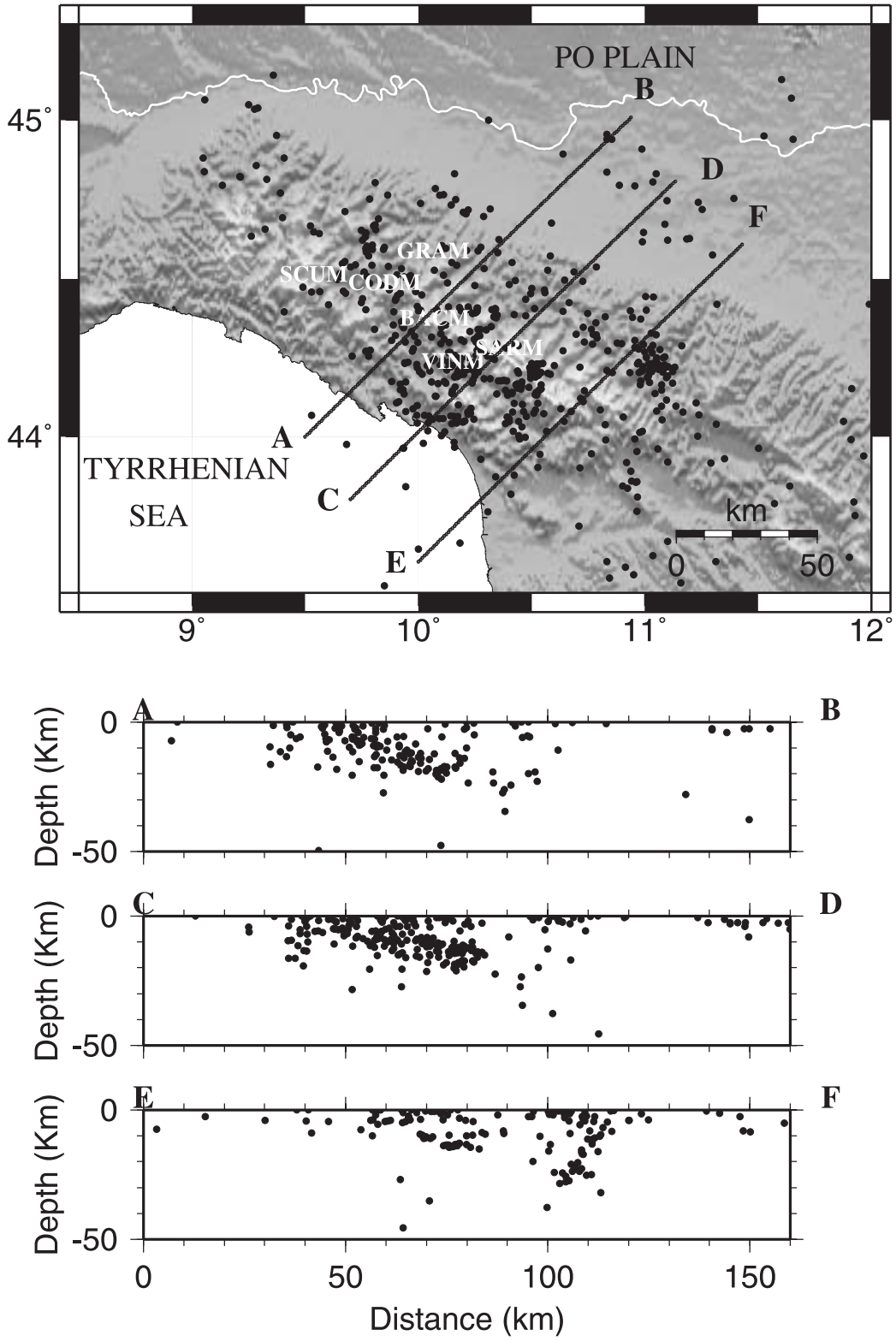
PO PLAIN
B
D
F
GRAM
SCUM
COLM
BACM
SAPM
VINM
A
C
E
TYRRHENIAN
SEA
km
0
50
45°
44°
9°
10°
11°
12°
A
B
C
D
E
F
Depth (Km)
0
-50
0
50
100
150
Distance (km)

Figure 3

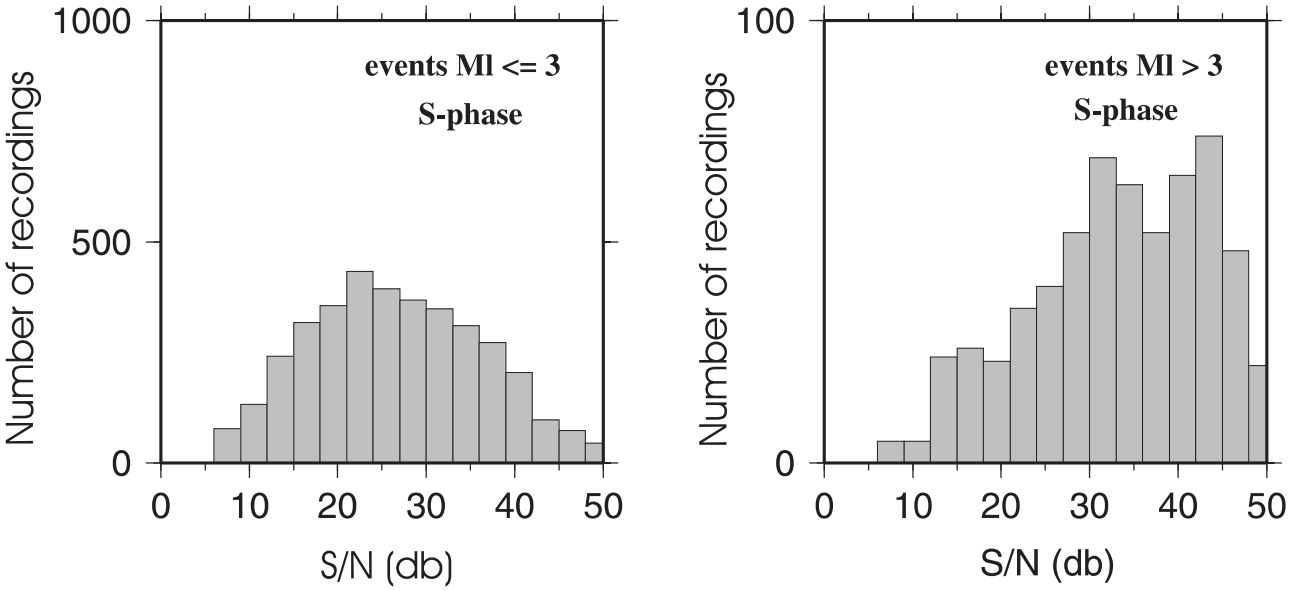
1000
500
0
Number of recordings
events Ml <= 3
S-phase
0
10
20
30
40
50
S/N (db)
100
0
Number of recordings
events Ml > 3
S-phase
0
10
20
30
40
50
S/N (db)

Figure 4

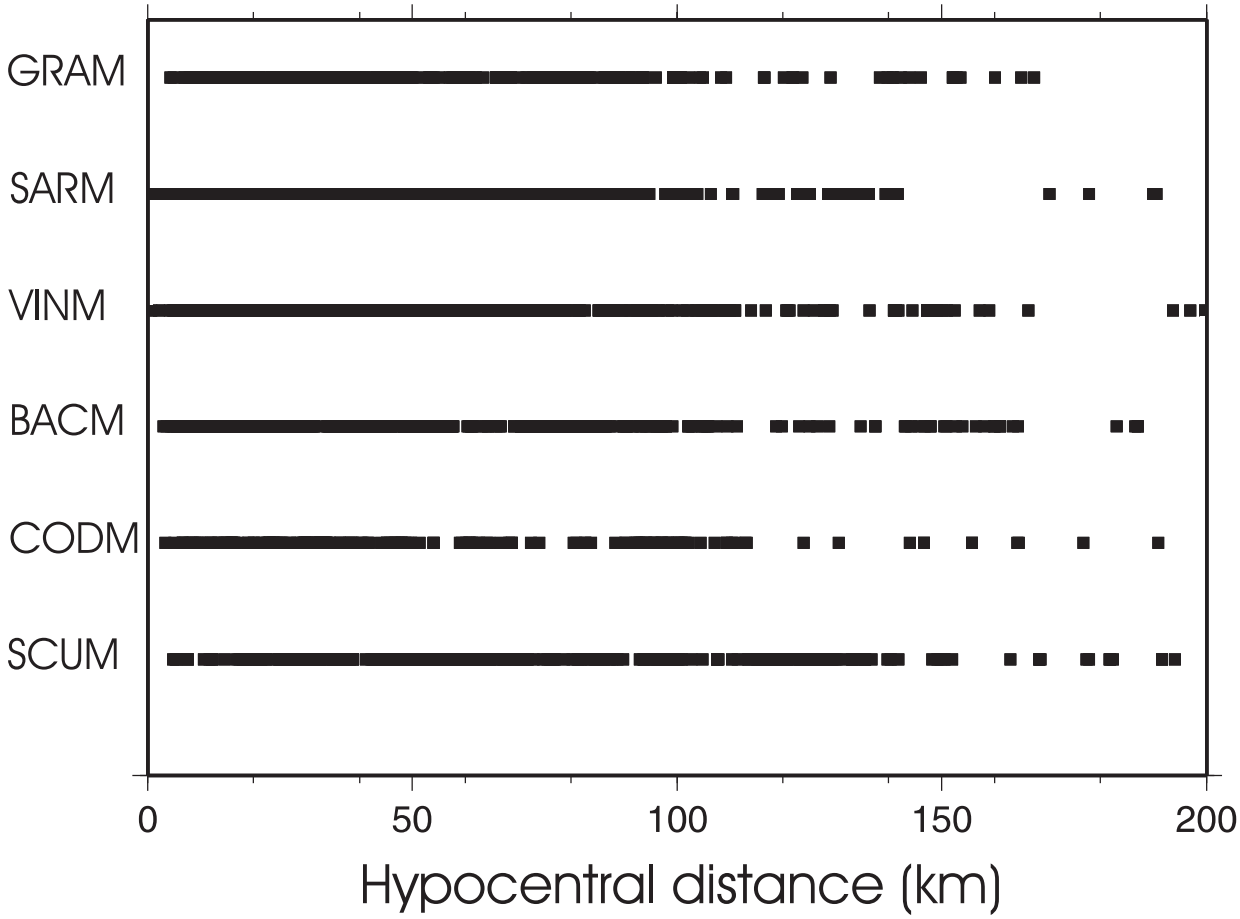
GRAM
SARM
VINM
BACM
CODM
SCUM
0
50
100
150
200
Hypocentral distance (km)

Figure 5

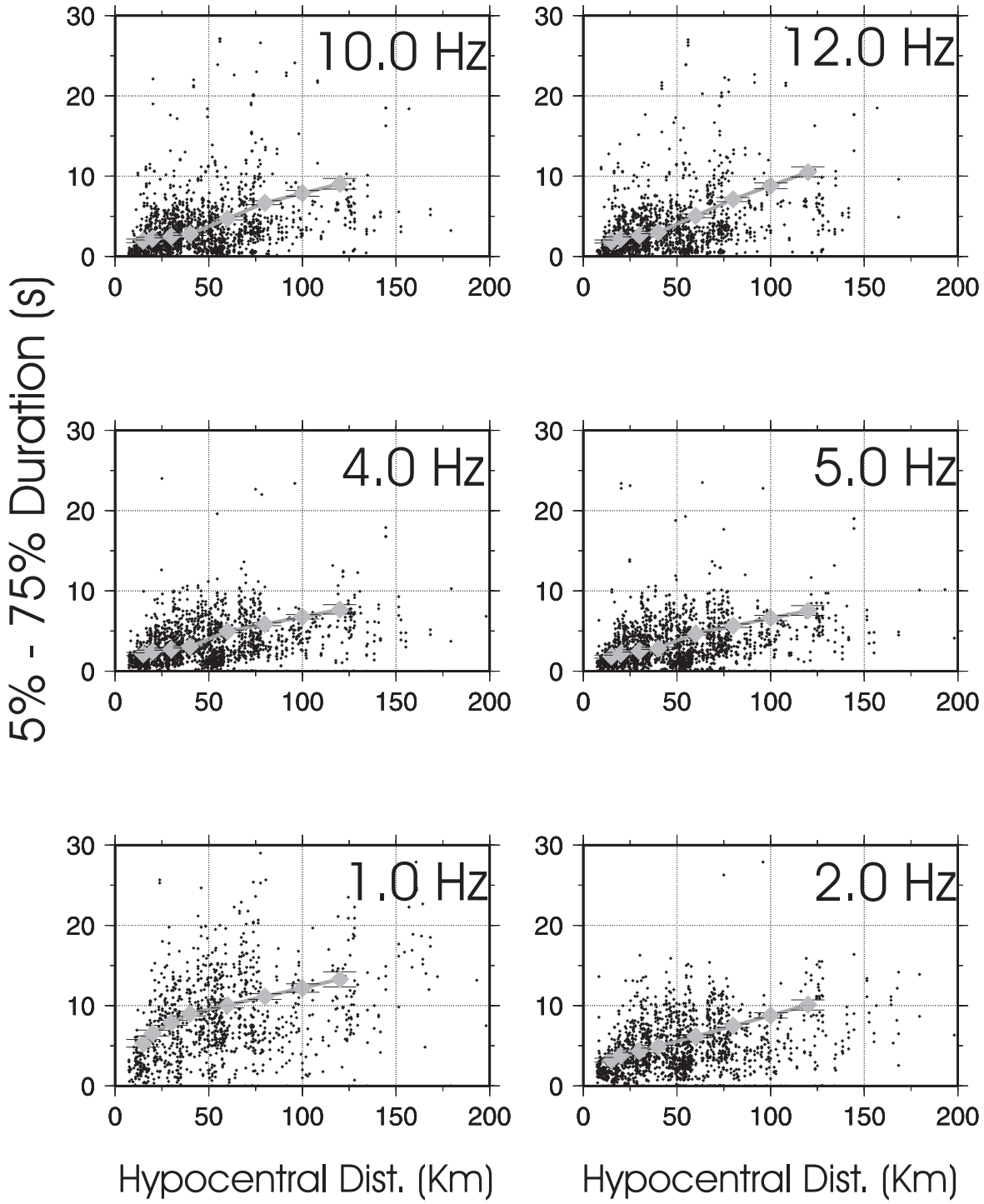
10.0 Hz
12.0 Hz
4.0 Hz
5.0 Hz
1.0 Hz
2.0 Hz
5% - 75% Duration (s)
Hypocentral Dist. (Km)
Hypocentral Dist. (Km)
0
10
20
30
0
50
100
150
200

Figure 6

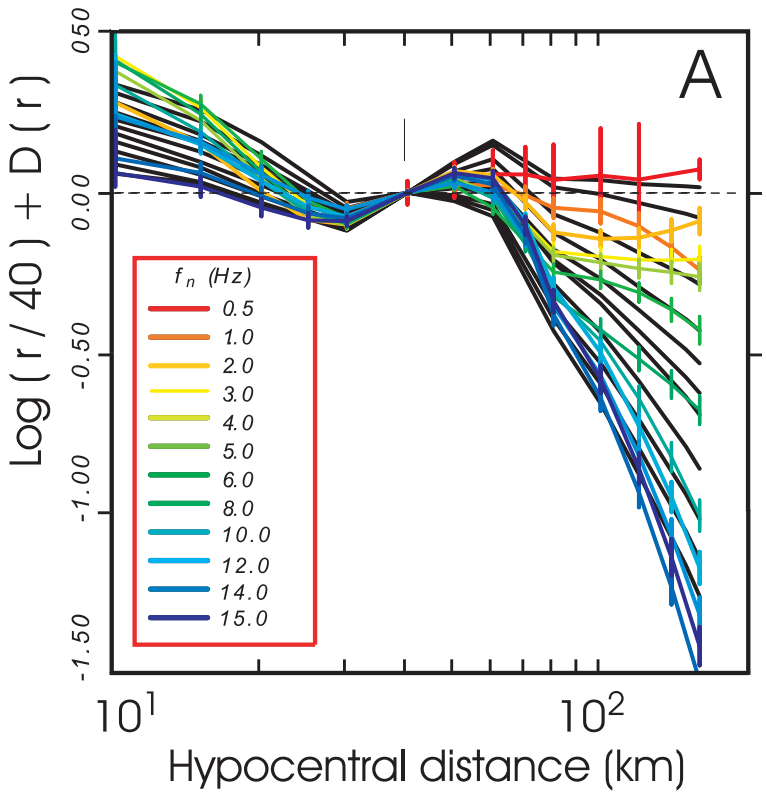
A
Log (r / 40) + D (r)
0.50
0.00
-0.50
-1.00
-1.50
f_n (Hz)
0.5
1.0
2.0
3.0
4.0
5.0
6.0
8.0
10.0
12.0
14.0
15.0
10^1
10^2
Hypocentral distance (km)

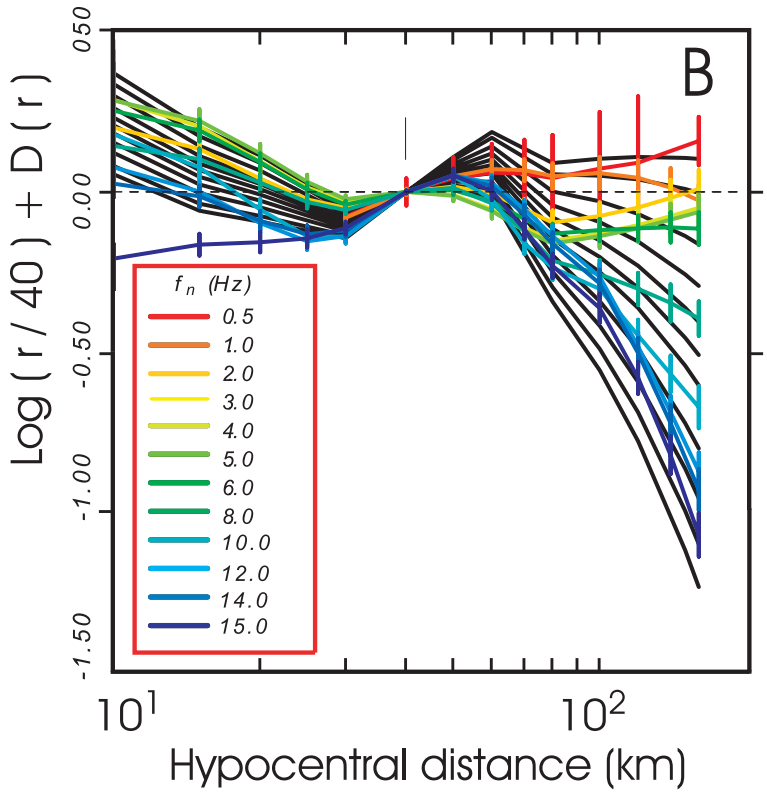
B
Log (r / 40) + D (r)
0.50
0.00
-0.50
-1.00
-1.50
f_n (Hz)
0.5
1.0
2.0
3.0
4.0
5.0
6.0
8.0
10.0
12.0
14.0
15.0
10^1
10^2
Hypocentral distance (km)

Figure 7

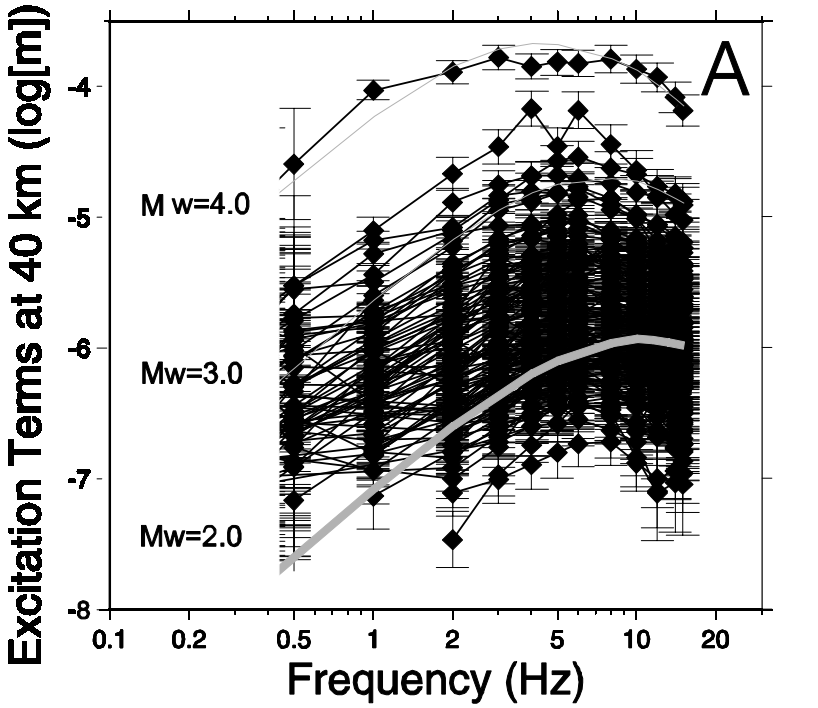
Peak Amplitudes Z-Comp.
A
M w=4.0
Mw=3.0
Mw=2.0
Excitation Terms at 40 km (log[m])
-4
-5
-6
-7
-8
0.1
0.2
0.5
1
2
5
10
20
Frequency (Hz)

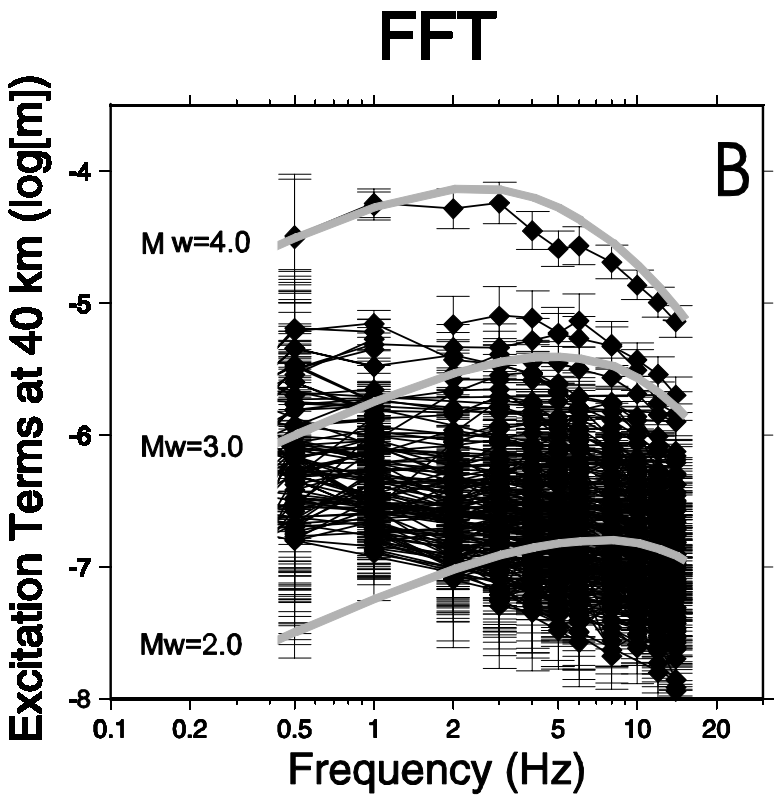
FFT
B
M w=4.0
Mw=3.0
Mw=2.0
Excitation Terms at 40 km (log[m])
-4
-5
-6
-7
-8
0.1
0.2
0.5
1
2
5
10
20
Frequency (Hz)

Figure 8

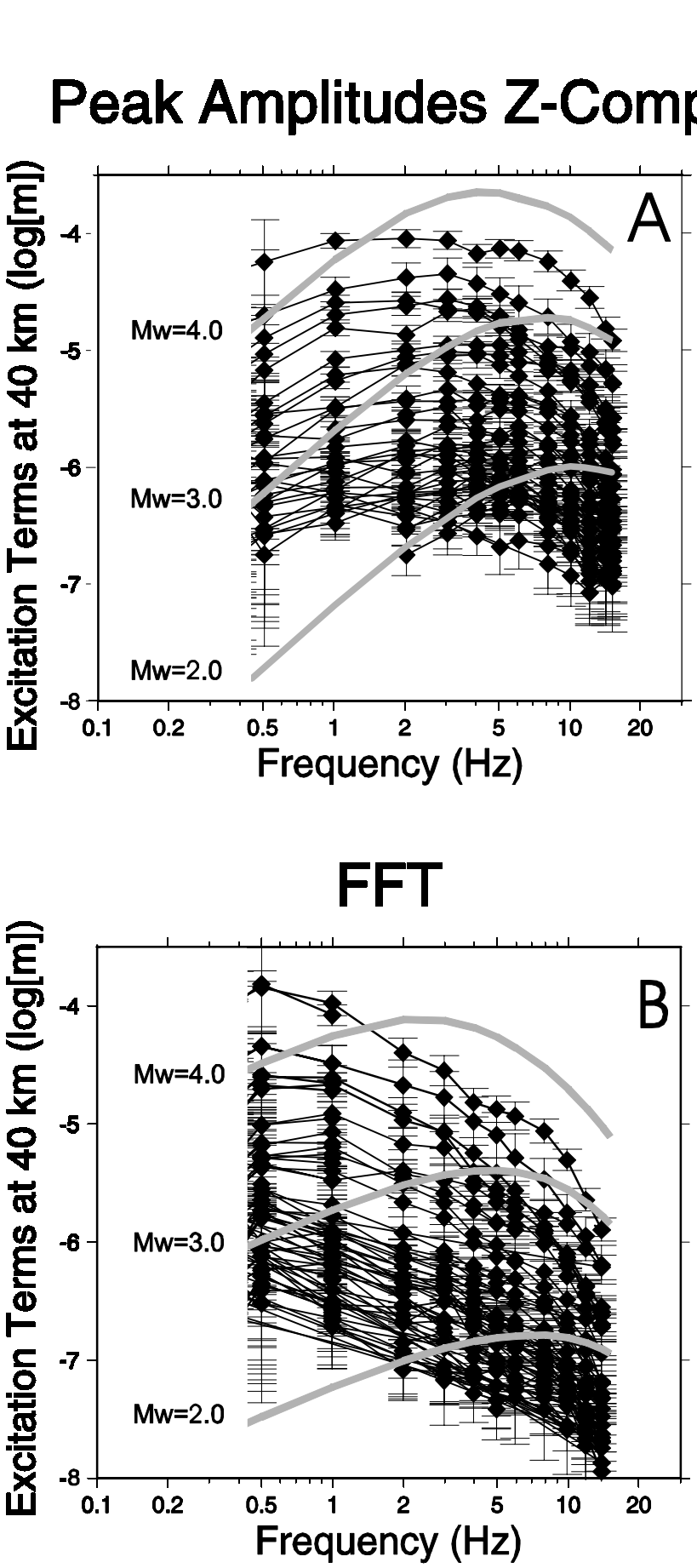
Peak Amplitudes Z-Comp.
A
Mw=4.0
Mw=3.0
Mw=2.0
Excitation Terms at 40 km (log[m])
-4
-5
-6
-7
-8
0.1
0.2
0.5
1
2
5
10
20
Frequency (Hz)
FFT
B
Mw=4.0
Mw=3.0
Mw=2.0
Excitation Terms at 40 km (log[m])
-4
-5
-6
-7
-8
0.1
0.2
0.5
1
2
5
10
20
Frequency (Hz)

Figure 9

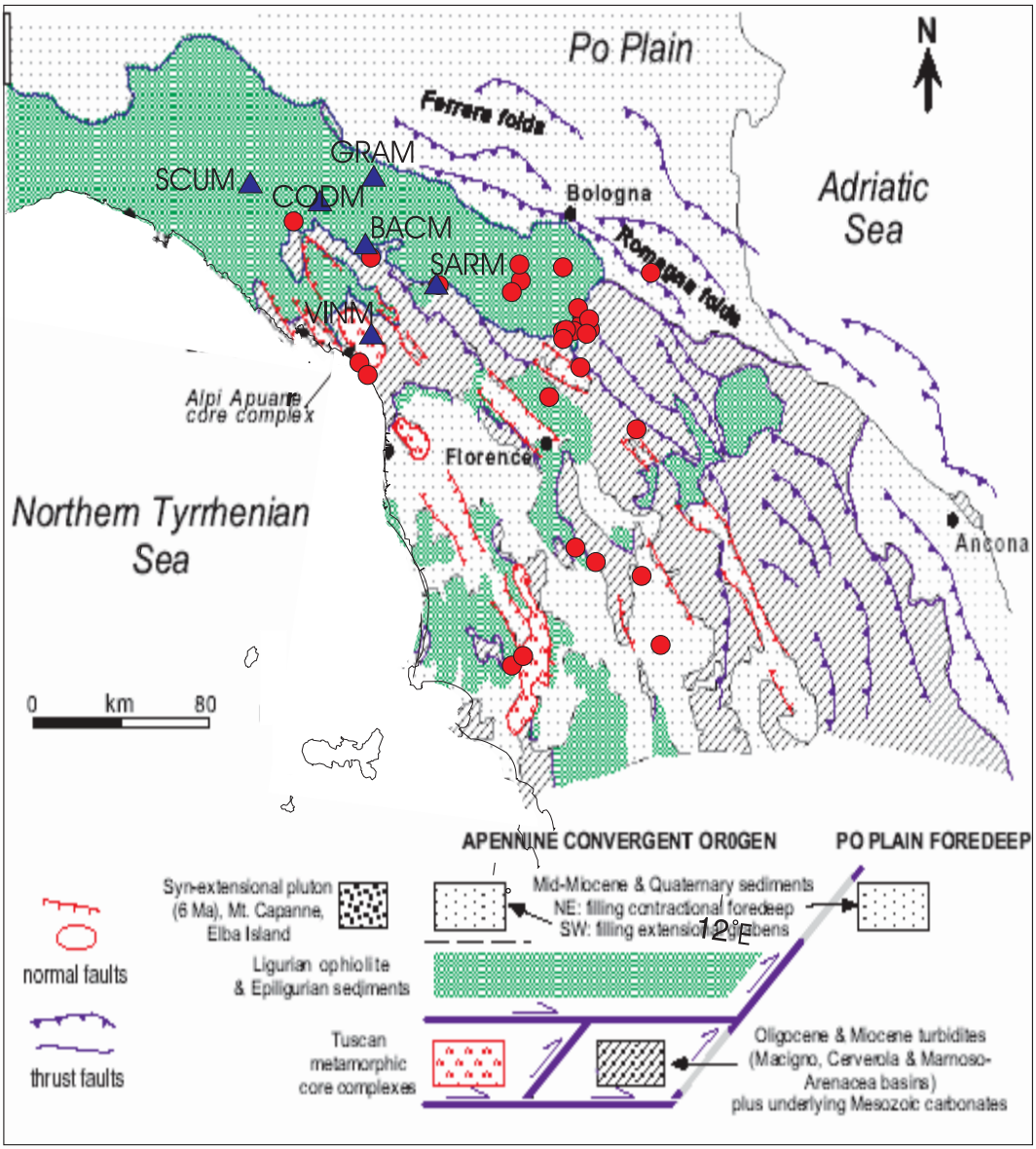
Po Plain
N
Ferrara folds
GRAM
SCUM
CODM
BACM
SARM
VINM
Bologna
Romagna folds
Adriatic Sea
Alpi Apuane core complex
Florence
Northern Tyrrhenian Sea
Ancona
0 km 80
APENNINE CONVERGENT OROGEN
PO PLAIN FOREDEEP
Syn-extensional pluton (6 Ma), Mt. Capanne, Elba Island
Mid-Miocene & Quaternary sediments
NE: filling contractional foredeep
SW: filling extensional grabens
12°E
normal faults
thrust faults
Ligurian ophiolite & Epiligurian sediments
Tuscan metamorphic core complexes
Oligocene & Miocene turbidites (Macigno, Cervarola & Marnoso-Arenacea basins) plus underlying Mesozoic carbonates

Figure 10

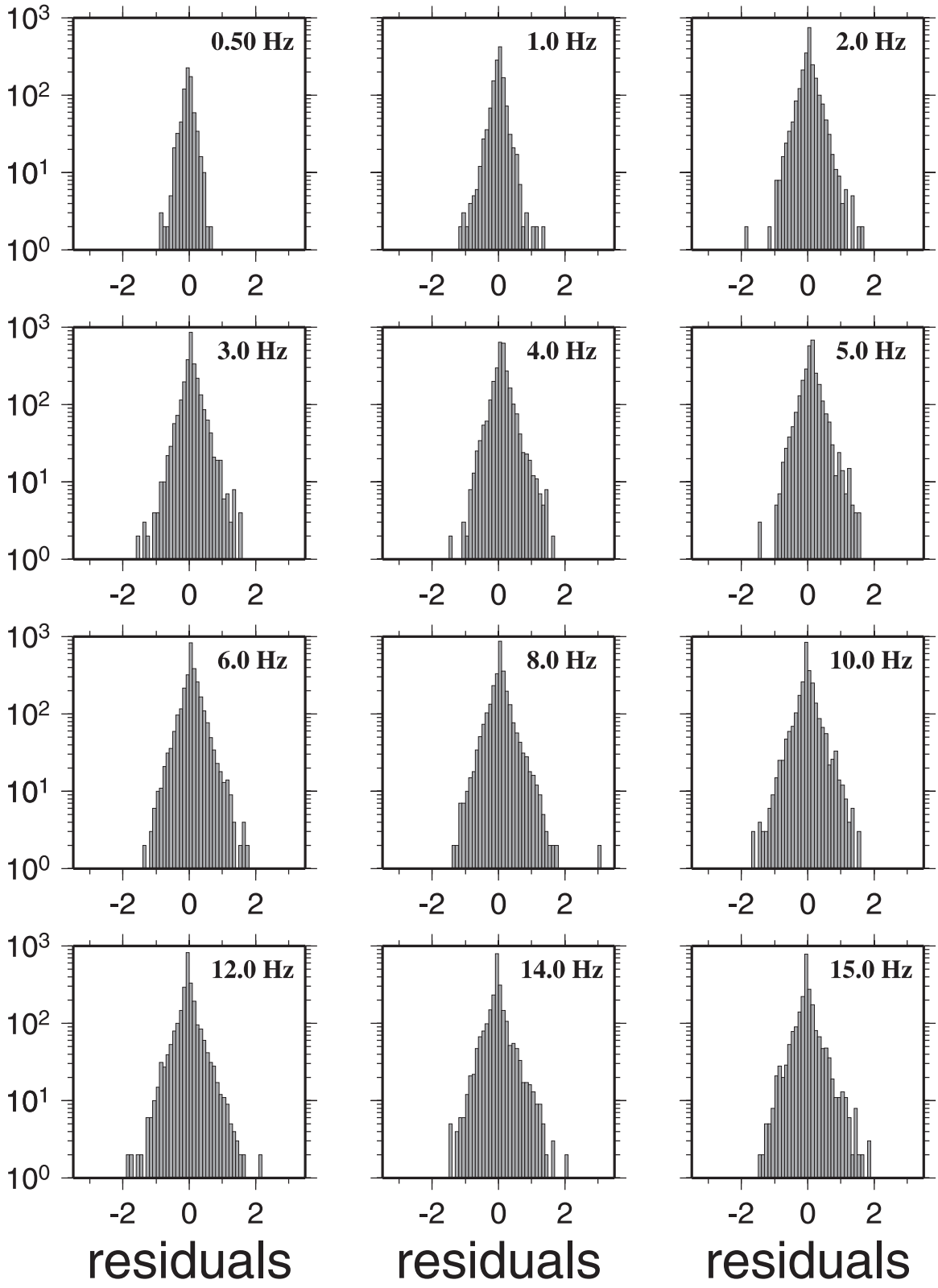
0.50 Hz
1.0 Hz
2.0 Hz
3.0 Hz
4.0 Hz
5.0 Hz
6.0 Hz
8.0 Hz
10.0 Hz
12.0 Hz
14.0 Hz
15.0 Hz
residuals
residuals
residuals

Figure 11

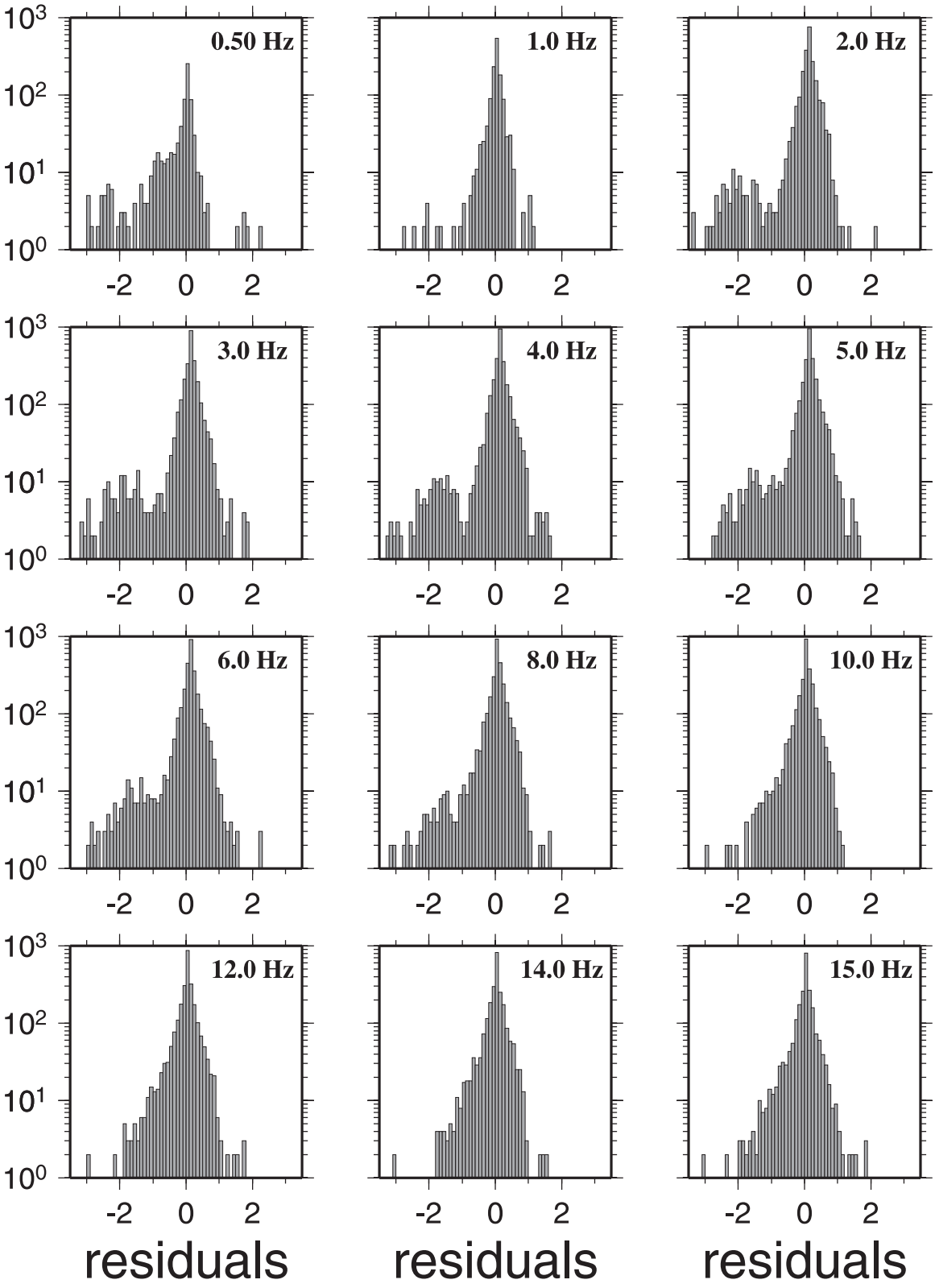
0.50 Hz
1.0 Hz
2.0 Hz
3.0 Hz
4.0 Hz
5.0 Hz
6.0 Hz
8.0 Hz
10.0 Hz
12.0 Hz
14.0 Hz
15.0 Hz
residuals
residuals
residuals

Figure 12

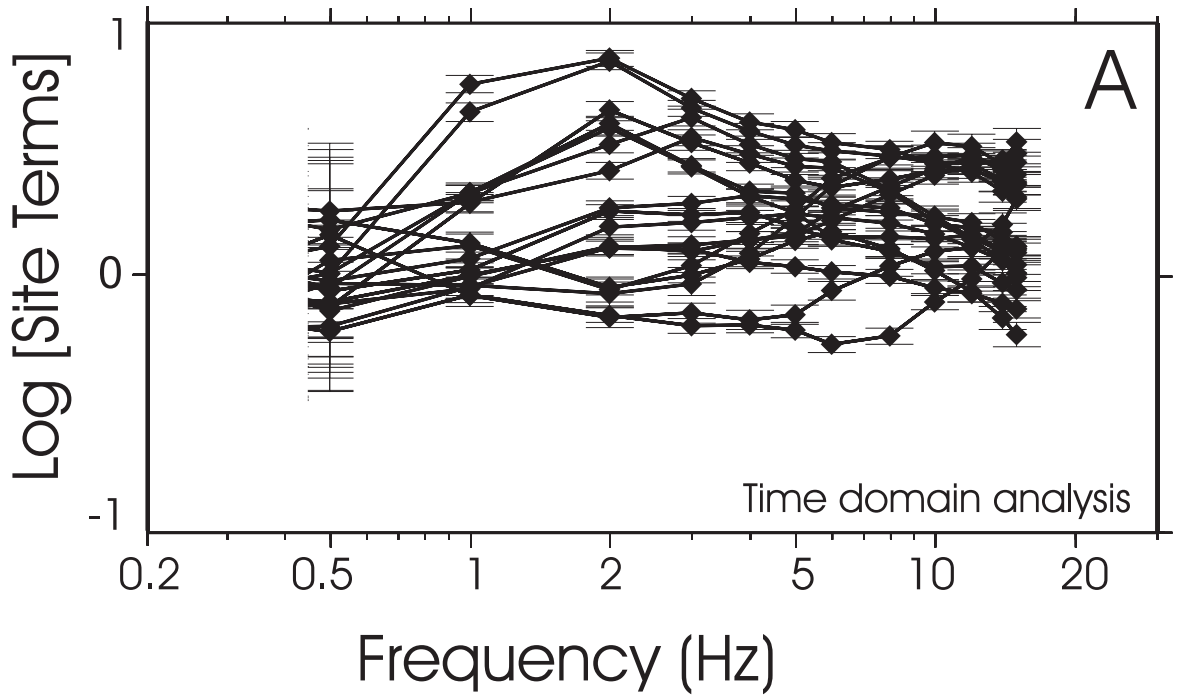
A
Log [Site Terms]
1
0
-1
0.2
0.5
1
2
5
10
20
Frequency (Hz)
Time domain analysis

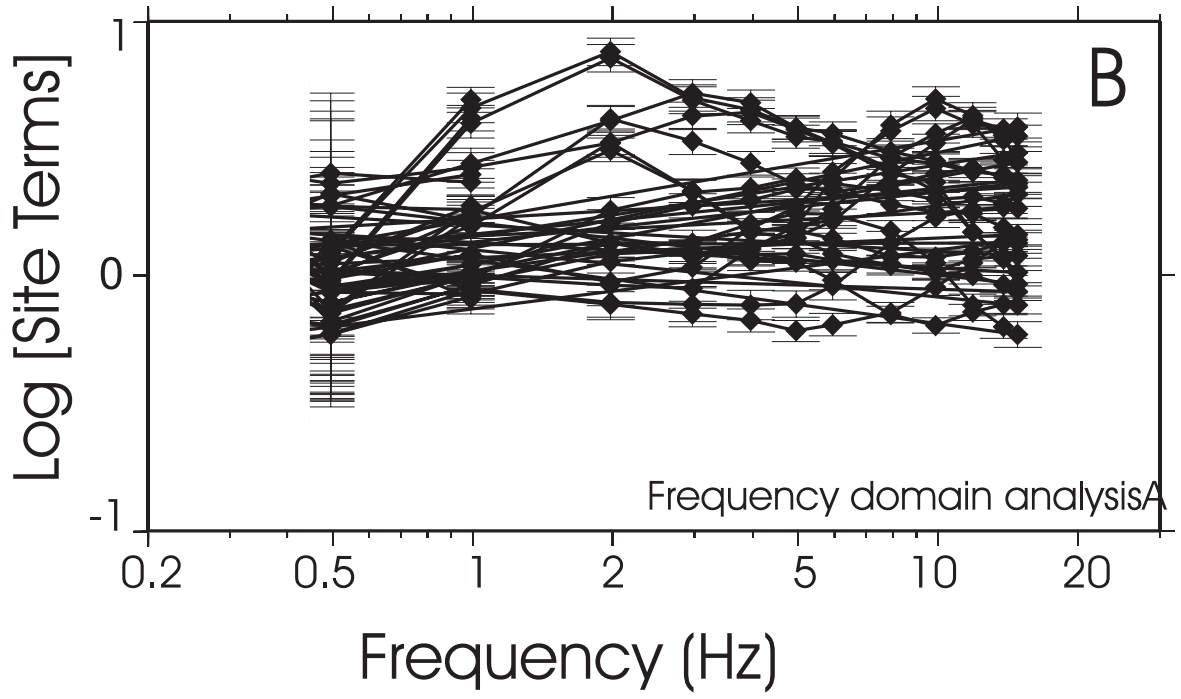
B
Log [Site Terms]
1
0
-1
0.2
0.5
1
2
5
10
20
Frequency (Hz)
Frequency domain analysisA

Figure 13

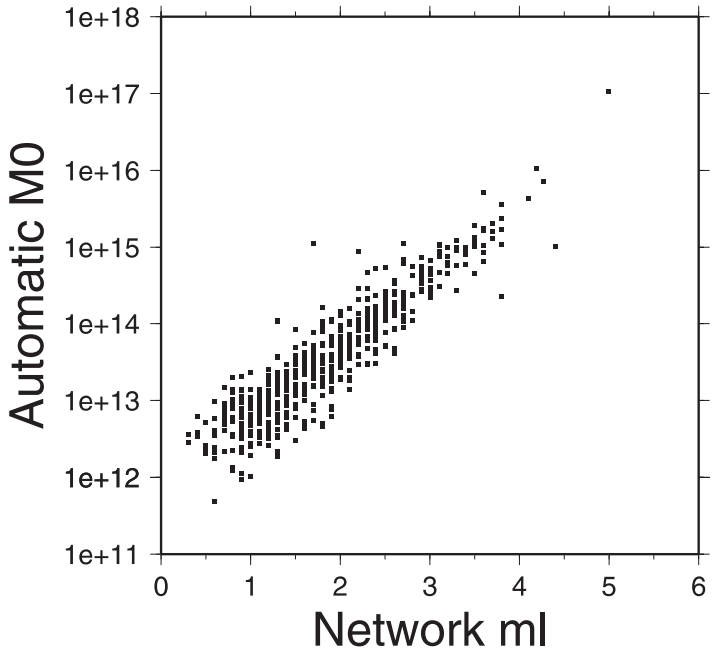
1e+18
1e+17
1e+16
1e+15
1e+14
1e+13
1e+12
1e+11
Automatic M0
0
1
2
3
4
5
6
Network ml

Figure 14

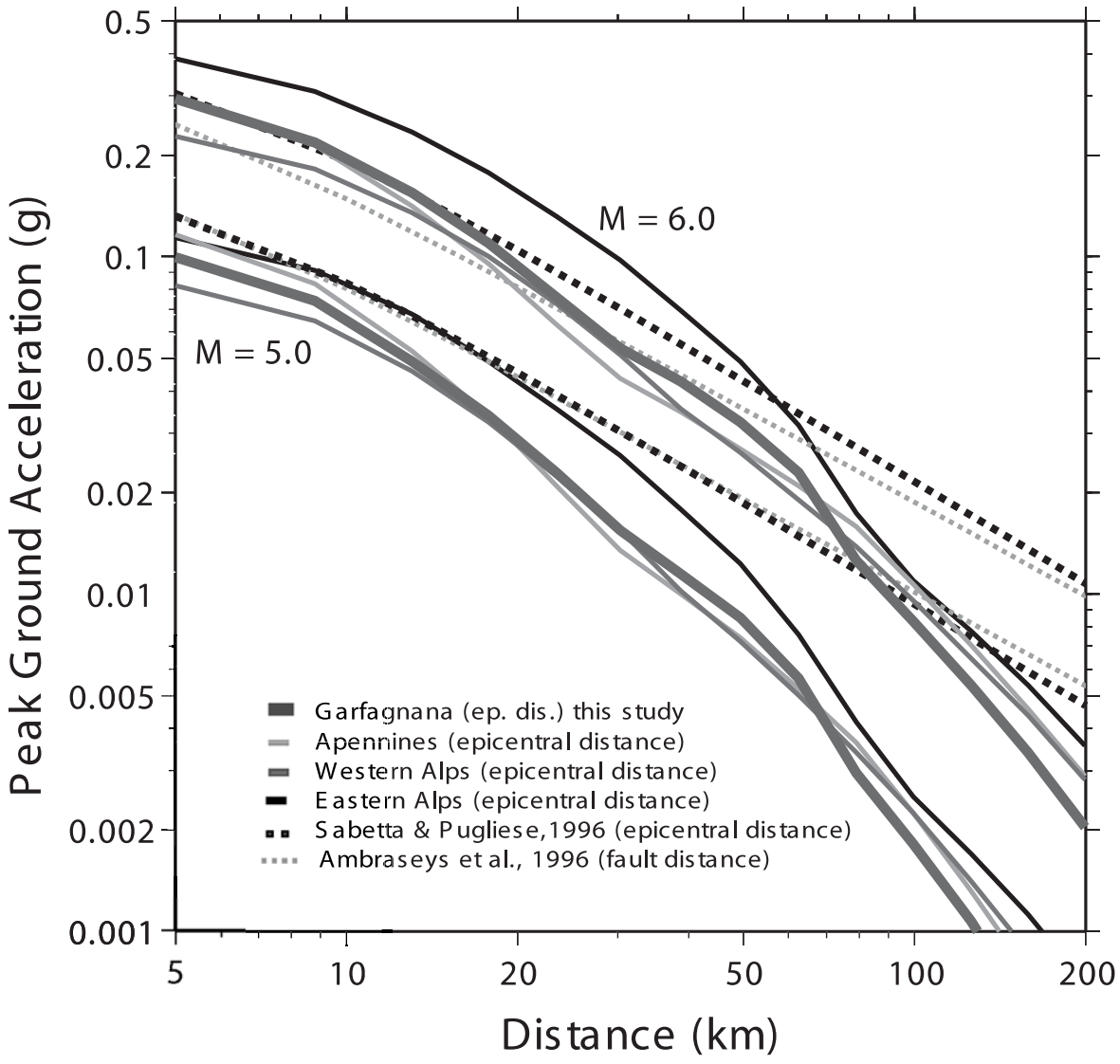
Peak Ground Acceleration (g)
0.5
0.2
0.1
0.05
0.02
0.01
0.005
0.002
0.001
M = 6.0
M = 5.0
Garfagnana (ep. dis.) this study
Apennines (epicentral distance)
Western Alps (epicentral distance)
Eastern Alps (epicentral distance)
Sabetta & Pugliese,1996 (epicentral distance)
Ambraseys et al., 1996 (fault distance)
5
10
20
50
100
200
Distance (km)

Figure 15